Fachtagung "Experimentelle Strömungsmechanik"
3. – 5. September 2019, Erlangen

Velocity measurement of a free jet in water with shear layer cavitation

Geschwindigkeitsmessung eines Freistrahls in Wasser mit Scherschichtkavitation

Julius-A. Nöpel[1], Erik Frense[1], Sarah Korb[1], Michael Dues[2], Frank Rüdiger[1]

[1]Institute of Fluid Mechanics (ISM), Technische Universität Dresden, Germany

[2]Intelligent Laser Applications Research and Development (ILA R&D) GmbH, Jülich, Germany

Key words: LDV-PS, free jet in water, hydrodynamic cavitation,
Schlagworte: LDV-PS, Freistrahl in Wasser, hydrodynamische Kavitation

Abstract

The paper presents a velocity measurement of a turbulent free jet in water with shear layer cavitation using a laser Doppler velocity profile sensor (LDV-PS). In this study, the influence of the cavitating bubbles on the measurement is investigated, but also different configurations regarding pressure difference are performed, determine the influence on the velocity value and measuring time. The evaluation of the raw data is explained and results of the velocity measurement for axial positions of the free jet are provided, as well as radial profiles. The axial data shows good agreement to numerical simulations and experimental data from the literature. There are differences between the radial profile and the literature, but explanations can be given in terms of uncertainties. It was found that the cavitating bubbles have a negative influence on the measurement in terms of time. However, the magnitude of the measured velocity at small bubble density corresponds to measurements of single-phase water flows. At very high bubble density, no more bursts are recorded, thus rendering the technique unusable in this case.

Introduction

The application of hydrodynamic cavitation in process engineering regarding the degradation of chemical substances has frequently been the subject of scientific investigations in recent years. In technical applications water accelerates strongly due to a constriction, which leads to a decrease in pressure. When the pressure drops below the vapour pressure of water, bubbles will grow and collapse as the pressure rises. Depending on the absolute pressure level, pressure difference, fluid and temperature, the density of the cavitating bubbles and their size changes.
The implosion of bubbles leads to extreme thermodynamic states, which cause homolytic cleavage of the water (Suslick et al., 1997). At the location of the collapse, the so-called hotspot, hydroxyl radicals arise. These radicals belong to the group of reactive electrophilic compounds, which react without preference with all electron-rich organic components (Stasinakis, 2008).

GALA e.V., Karlsruhe, Germany, ISBN 978-3-9816764-6-4

The motivation for using cavitation lies in the fact that chemical substances present in water can be oxidized without using additional chemicals. However, previous research did not consider the local conditions of the multiphase flow, especially in the bubble field. Different groups measure substance concentrations only before and after treatment by cavitation (Mishra and Gogate, 2010).
In this article, the measurement of local conditions in terms of velocities is conducted using a Laser Doppler velocity profile sensor. The influence of the bubbles on the experiments as well as the characteristics of the measurement method will be investigated . The recorded local velocities will be used later for the validation of numerical models. In addition, the in-situ conditions in the reactor are of great interest for experimental degradation tests and design optimization. The measurement is performed in the area of the shear layer cavitation of the turbulent free jet. Figure 1 shows different bubble regions for a pressure difference of Δp = 20 bar. By increasing the pressure at the outlet of the reactor p_2, the bubble density can be significantly reduced.

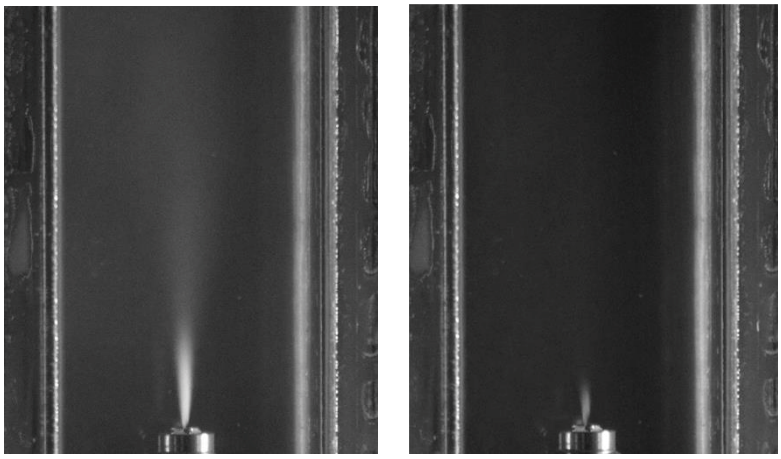

Figure 1: Cavitating free jet flow with nozzle diameter d = 0.6 mm inside the reactor at pressure difference Δp = 20 bar. Left: Inlet absolute pressure p_1 = 21 bar and p_2 = 1 bar. Right: Inlet absolute pressure p_1 = 22 bar and p_2 = 2 bar.

The series of measurements will be used to investigate the influence of the existing bubbles on the velocity, but also on the measurement time. The axial and radial data obtained will be compared with numerical data and experimental data from the literature.

Experimental setup

The experimental setup is shown in Figure 2 including an adjustable high-pressure pump (1) performing maximum volume flow rate of $\dot{V}_{max}$ = 10 l/min and operating pressure up to p_{max} = 170 bar. Deionised water flows through a nozzle with d = 0.6 mm into the acrylic glass cavitation reactor (2) characterized by a square cross-sectional area of A = 900 mm². The water temperature is kept sufficiently constant at values of T = (25 ± 5) °C via a cooling coil located in the open tank (4). The systems total fluid volume is V = 2.5 l. Besides that, the whole pipe system consists of parts made of stainless steel. Manometers are installed to measure the absolute pressure p_1 upstream of the nozzle at the high-pressure section of the system as well as the relative pressure downstream of the reactor chamber from which the pressure p_2 is taken. The manual adjustment of the valve (3) affects the pressure inside the reactor chamber. Silver-coated hollow glass spheres with a diameter of d_p = 13 µm are used as seeding material.

GALA e.V., Karlsruhe, Germany, ISBN 978-3-9816764-6-4

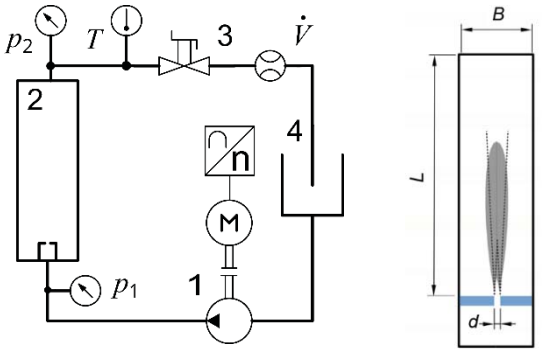

Name	Symbol	Value [mm]
Nozzle diameter	d	0.6
Reactor chamber width	B	30
Reactor length	L	150

Figure 2: Experimental setup of the hydraulic circuit and sketch of the cavitation reactor with main dimensions. 1 – high-pressure pump, 2 – cavitation reactor, 3 – valve, 4 – open tank with cooling coil.

Conditions of investigation

The flow in the reactor is investigated at different points of operation, see Table 1. By selecting different pressure differences and pressure levels at the reactor outlet, the influence of velocity on the measurement, bubble density and required measurement time could be investigated.

Table 1: Overview of investigated operating points and labelling.

Name	Supply pressure p_1 [bar]	Outlet pressure p_2 [bar]	Pressure Difference Δp [bar]	Nozzle exit velocity w_d [m/s]
0601	6	1	5	29.5
1101	11	1	10	41.3
1202	12	2	10	41.3
2101	21	1	20	54.2
2202	22	2	20	54.2

The respective experiment is labelled by a four-digit number, which indicates the different pressure boundary conditions. The digits represent first the inlet pressure p_1 and last the outlet pressure p_2. Increasing the outlet pressure p_2 causes a stronger collapse of the bubble due to a higher positive pressure gradient in the direction of flow. This leads to a reduction of the bubble density in the reactor, as it is shown in Figure 3.

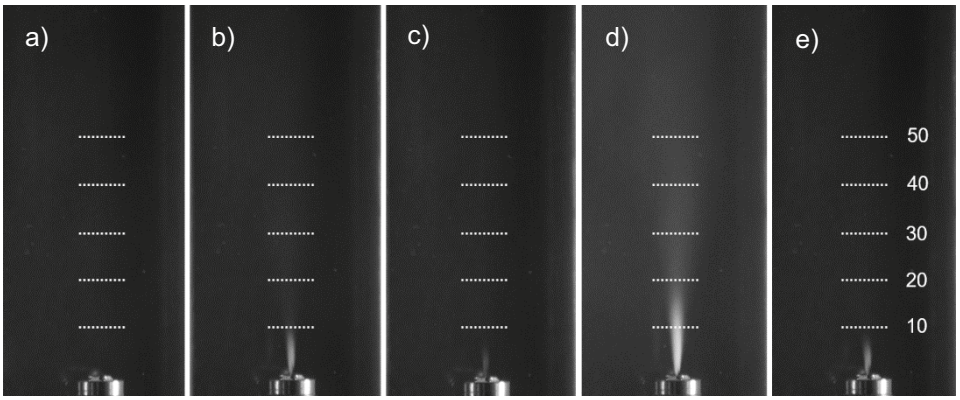

Figure 3: Overview of the different flow conditions in the reactor recorded by single-lens camera at exposure time of t_p = 10 ms. a) 0601 – Labelled by pressure p_1 = 6 bar and p_2 = 1 bar as absolute pressure values, b) 1101, c) 1202, d) 2101, e) 2202. The dotted lines in the pictures represent the axial measuring positions. These are in the range from x/d = 10 to 50.

GALA e.V., Karlsruhe, Germany, ISBN 978-3-9816764-6-4

Table 1 lists the nozzle exit velocities for the three different pressure differences. In addition, it must be assumed that these cross-sectional averaged velocities are subject to a fluctuation margin of at least 10 percent.

Measurement technique and data evaluation

In Terms of laser Doppler velocimetry, LDV-PS has been developed adding a second pair of laser beams with a distinguishable wavelength forming an additional measuring volume in the same plane. A complete overview of the method can be found in Czarske et al., 2002. LDV-PS is able to measure both, velocity and the position of a particle passing through the measurement volume. The used commercial LDV-PS (ILA R&D GmbH) is characterized by two beam pairs with waveleght of 532 nm and 561 nm, a focal length of 160 mm, a measurement volume length of l_{MV} = 400 µm and a spatial resolution of Δy = 5 µm. Figure 4 shows the setup.

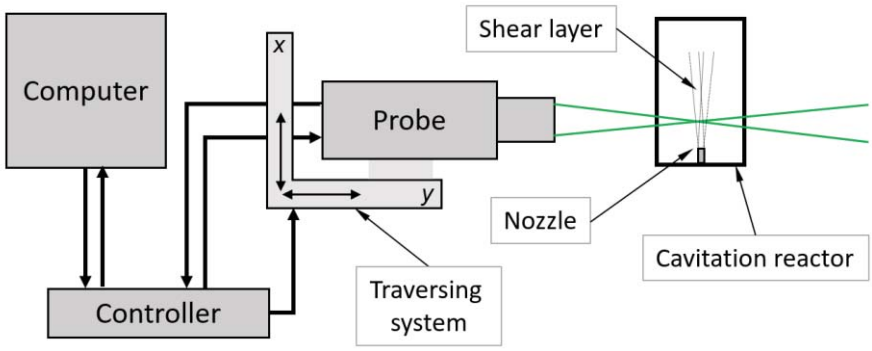

Figure 4: Setup of the measurement technique with the cavitation reactor and the traversing system.

The recorded raw data have information about the frequency and the fringe distance at the location of the particle crossing in the measuring volume. From this, the velocity of the tracked particle is determined. All configurations evaluated here have a minimum burst count of N = 100,000 per measuring point to ensure statistical significance of the data. Only for the radial measurement of 1101 the burst amount criterion was set to N = 25,000 bursts because of the extremely low burst rate. No software filters were used so that the same setup could be used for all measurement points. After the measurement, the raw data can be checked and edited before filtering and averaging.

In terms of data evaluation, recorded bursts are divided into classes. The number of classes is 100 bins per measurement volume out of which the mean value and the standard deviation can be calculated. The measurement data is filtered by a threshold for the velocity and the spatial position. This applies to classes with a number of bursts less than 10 % of the maximum number of bursts per class in the measuring volume.

This is done to exclude erroneous bursts caused by bubble reflections or if there are only very few data in the edge classes of the measurement volume that are not statistically reliable. Physically, the light intensity in the outer area of the measuring volume is weaker, whereas the backscattered light from the particles must be weaker and can be poorly absorbed by the photodetector with the appropriate path and refraction.

After filtering, the respective mean velocities are formed for each class and plotted over the length of the measurement volume. For the radial measurement of the velocity, the measuring volume is traversed while overlapping in order to obtain a higher number of bursts in the outer areas of the measuring volumes.

The laser beam is refracted at the interfaces. Because the relative zero point is located at the outlet of the nozzle inside the reactor, only the refractive index of the water ε = 1.33 has to be used to scale the beam axis coordinate. However, the fringe distance remains unaffected.

GALA e.V., Karlsruhe, Germany, ISBN 978-3-9816764-6-4

Results of measurement

Axial velocity at the centerline

The results of the normalised axial velocity at the centerline for all investigated configurations are shown in Figure 5. The data are compared with experimentally determined data from a single-phase water flow, which is listed as an empirical function from Bollrich et al., 1989. In addition, data of the averaged flow velocity from a RANS simulation with ANSYS Fluent 19 with cavitation multi-phase model are displayed at Δp = 10 bar for comparison.

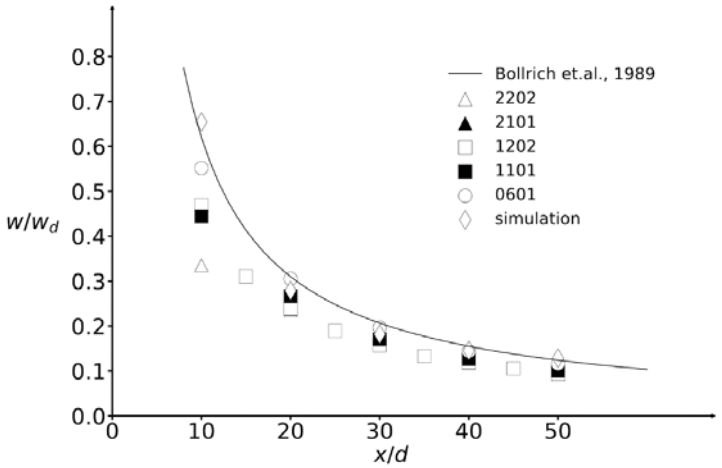

Figure 5: Average axial velocity of the free jet in water for different positions x/d. Comparison of the acquired LDV-PS data with own numerical data, as well as empirical data for single-phase jet from Bollrich et al., 1989.

The measured velocities are normalized with the nozzle exit velocity w_d. The distance x in the axial direction on the jet axis is normalized with the nozzle diameter d. This ensures the possibility of comparing the data under the condition of similarity, which is typical for free jet configurations. First of all, the data are for the most part quite close to the literature values according to Bollrich et al, 1989. This is particularly noticeable in the range from x/d = 30, whereby the points are converging with increasing distance. The closer the measurement was carried out to the nozzle outlet at x/d = 0, the higher the deviation between the measurements become. The largest deviation is found for 2202 at x/d = 10, whereby 1101 and 1202 are also below the theoretical curve at similar velocities. The bubble area lengths shown in Figure 3 above reveals that 1101 leads to the second longest bubble area, followed by 2202 and 1202. The bubbles seem to lead to an increased number of faulty bursts, which falsifies the statistics of the data. The highest deviation at 2202 is due on the one hand to the bubble influence and on the other hand to the higher nozzle exit velocity. Due to fluctuation, velocities close to or above the upper-velocity limit of the used LDV-PS system of w_{max} = 40 m/s are reached. This means that these events cannot be recorded in the measurement and therefore do not appear in the burst statistics. This causes a shift of the average speed to lower levels. For the measurement 2101, no bursts could be recorded at x/d = 10. This is due to the strongly increased bubble density, as can be seen in Fig. 3d.
The measurement 0601 with a small pressure difference shows a high agreement to the literature data as well as to the numerical data over the entire range. However, it should be noted that the single-phase literature data are compared to a multiphase flow that is present in any case. The data from a numerical simulation correspond well with the empirical literature data. This is due to the fact that the simulation values reflect a stationary, single-phase flow, whereby no cavitation model is used.

GALA e.V., Karlsruhe, Germany, ISBN 978-3-9816764-6-4

There are also geometrical and technical uncertainties which can lead to a discrepancy. Firstly, due to the manufacturing tolerance of the nozzle, a deviation of $\Delta\tilde{d}$ = +0.02 mm can be assumed. In addition to this, the accuracy class of 1.6 corresponding to errors from the manometer, as well as reading errors are added.
The uncertainty of the measured value of the manometer is thus $\Delta\tilde{p}$ = ± 1.96 bar. Errors of up to 10 % are to be expected when determining the volume flow rate. In the case of maximum volume flow, the error is in the range of $\Delta\tilde{\dot{V}}$ = 0.09 l/min. The error size which is decisive for normalization is consequently the nozzle exit velocity w_d, which is calculated from the volume flow divided by the cross-sectional area of the nozzle. It turns out that the uncertainty of the nozzle exit velocity for Δp = 10 bar is in the range of $\Delta\tilde{w}_d/w_d$ = 13 %.
Figure 6 shows the measurement time t for all measurements over the axial positions x/d in order to achieve a count of N = 100,000 bursts. The concentration of seeding particles in the liquid is kept constant. For operating point 0601, the shortest measurement time is consistently determined. This is due to the almost bubble-free flow at comparatively low speed. The measurement at Δp = 10 bar is similar for positions above x/d = 10. At x/d = 10, more bubbles occur, as can be seen in figure 3. For the higher bubble-loaded flow 1101, three times the measurement time is required compared to 1202, whereby the average velocity is similar. For configuration 2101, no data recording could be accomplished at x/d = 10, whereby even at x/d = 20 the bubble density is still very high (Fig. 3d). This leads to a high measurement time. For 2202 at x/d = 10, similar to 1202, increased measuring times due to the bubble area can be observed. For the further values of 2202, the measuring time is similar to the other configurations. In general, the trend can be seen, especially for 0601, that the higher the velocity, the shorter the recorded measurement times are, if the bubble influence is small and the particle velocity is below the maximum LDV-PS velocity. This is due to the particle velocity on the one hand and on the other hand to the particle concentration, which spreads out with increasing distance from the nozzle with jet expansion, leading to longer measuring times in conjunction with an additional decrease in velocity.

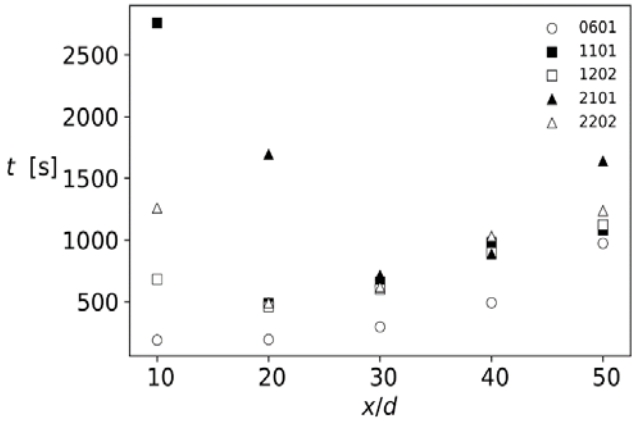

Figure 6: Measurement time t for acquiring N = 100,000 bursts for each configuration for the same amount of seeding particles in the liquid.

Radial profile of axial velocity

The total amount of bursts acquire with the LDV-PS for one operating point can be seen in Figure 7. In the histogram on the left the separation into different classes, from which mean values and standard deviation are calculated is shown. The right plot shows the order of the deviation of the measuring system. The white line characterises the mean velocity at the corresponding position. The mean velocity of the classes was calculated from the raw data of the overlapping measurement.

GALA e.V., Karlsruhe, Germany, ISBN 978-3-9816764-6-4

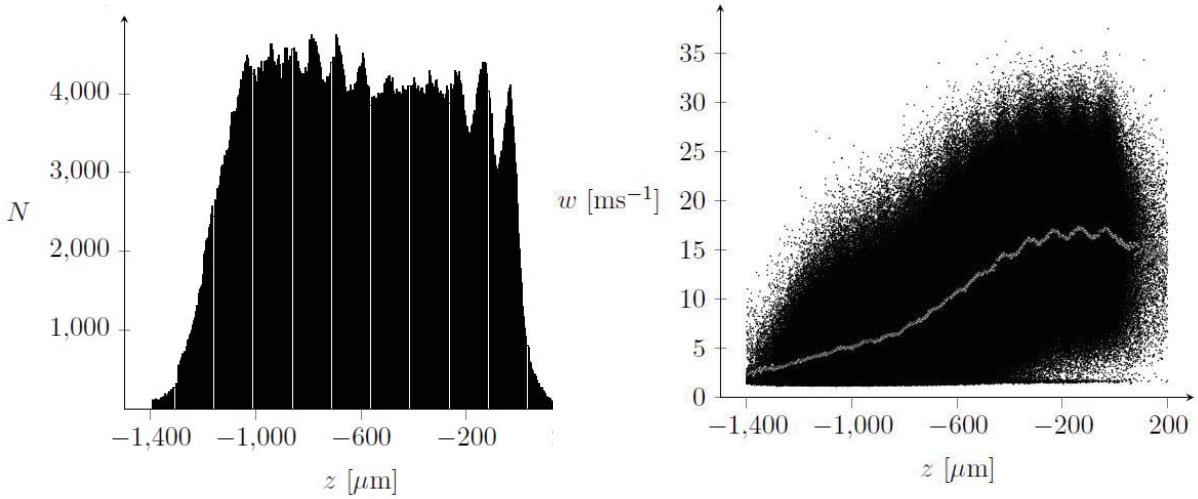

Figure 7: Total amount of bursts acquired with the LDV-PS at x/d = 10 with Δp = 10 bar. Left.: Histogram of bursts detected at various locations. Right: Scatter diagram of every burst plotted as a dot.

Figure 8 shows the results of the radial measurement at x/d = 10 with a pressure difference of Δp = 10 bar. In the radial range, the measurements resulted in lower velocities than in the literature. In this plot the profile 1202 contains the velocity values which were measured traversing the measurement volume in y-direction, as for conventional LDV perpendicular to the optical axis. This enables to find out the maximum velocity within the measurement volume and thus to compensate uncertainties in the positioning

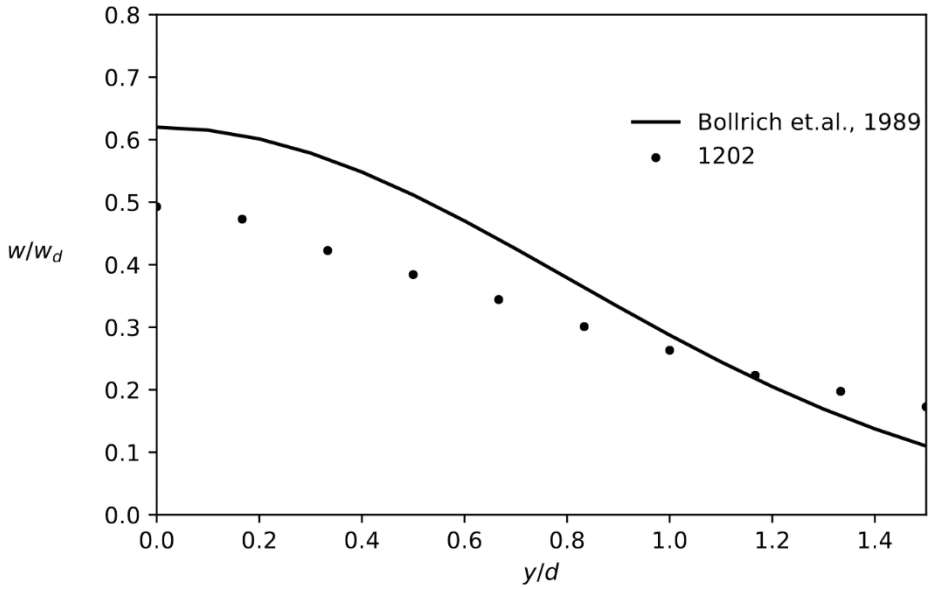

Figure 8: Average radial velocity of the free jet with cavitation in water for x/d = 10 at Δp = 10 bar with data points of 1202 obtained by traversing perpendicular to the optical axis and the empirical correlation for single-phase jet from Bollrich et al., 1989.

The profiles sampled by traversing along the optical axis show strong deviations and were not plotted in Figure 8. A number of effects has to be investigated in detail before presenting these results. In principle, uncertainties similar to the axial measurement at centerline are to be mentioned here. First, the position of the measuring volume in relation to the nozzle outlet is subject to uncertainty. Especially in the dimension range of the free jet with a nozzle outlet diameter

GALA e.V., Karlsruhe, Germany, ISBN 978-3-9816764-6-4

of d = 0.6 mm, micrometre displacement from the jet axis has a strong effect. In addition, manufacturing tolerances of the nozzles, which can cause an inclination of the jet, must be mentioned in this context. In addition, large bubbles in the secondary flow crossing the laser beam influence the postion of the measurement volume. The values measured here contain the absolute velocity. A LDV-PS with shifting could be used to obtain the direction of velocity.

Concluding remark

In this paper, velocity measurements on a turbulent cavitating free jet with LDV-PS were successfully performed. It was possible to show the influence of the bubbles on the measurement by means of the measurement times and the axial profiles. In addition, at x/d = 10 radial profiles could be recorded. It became clear that even small deviations between the very small spatial expansions of the jet and the geometry to the very high velocities and the gradients in the jet have large effects on the measurement result. Uncertainties were mentioned and have to be analysed in detail in future investigations.

Acknowledgements

This work was supported by the federal ministry for economic affairs and energy (BMWi) on the basis of a decision by the German Bundestag (16KN073422).

Literature

Bollrich, G. et al., 1989: “Technische Hydromechanik /2”, VEB Verlag für Bauwesen, Berlin.
Czarske, J., Büttner, L., Razik, T., Müller, H., 2002: “Boundary layer velocity measurements by a laser Doppler profile sensor with micrometre spatial resolution”, Measurement Science and Technology, Vol. 13, No. 12, pp. 1979-1989.
Mishra, K.P., Gogate, P., 2010: “Intensification of degradation of Rhodamin B using hydrodynamic cavitation in the presence of additives”, Journal of Separation and Purification Technology, Vol. 75, pp. 385-391.
Nöpel, J.-A., Zedler, P., Deggelmann, M., Braeutigam, P., Fröhlich, J., Rüdiger, F., 2018: “Experimental investigation of the bubble distribution and chemical reactions induced by hydrodynamic cavitation inside a reactor – a preliminary study”, Conference Proceedings 5th ICEFM, Munich, 679–684.
Stasinakis, A.S., 2008: “Use of selected advanced oxidation processes (AOPs) for wastewater treatment – A mini review”, Global Nest Journal, Vol. 10, No. 3, pp. 376-385.
Suslick, K.S., Mdleleni, M.M, Ries, J.T, 1997: “Chemistry Induced by Hydrodynamic Cavitation”, Journal of the American Chemical Society, 119, pp. 9303-9304.

GALA e.V., Karlsruhe, Germany, ISBN 978-3-9816764-6-4